

2 f
NASA CR-130119

STAR

DEVELOPMENT OF AN INFRARED POLARIMETER

David L. Coffeen
Lunar and Planetary Laboratory
University of Arizona
Tucson, Arizona 85721

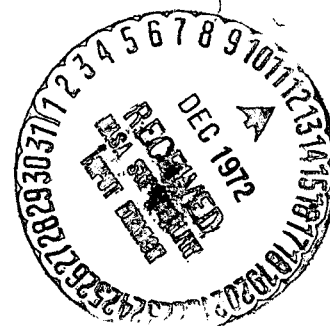
October 1972

Final Project Report for Period September 71 - September 1972

Prepared for:

GODDARD SPACE FLIGHT CENTER

Greenbelt, Maryland 20771



(NASA-CR-130119) DEVELOPMENT OF AN
INFRARED POLARIMETER Final Project Report,
Sep. 1971 - Sep. 1972 D.L. Coffeen
(Arizona Univ., Tucson.) Oct. 1972 28 p

N73-12458

Unclas

CSCCL 14B G3/14 48833

Reproduced by
NATIONAL TECHNICAL
INFORMATION SERVICE
U S Department of Commerce
Springfield VA 22151

27
27

1. Report No.	2. Government Accession No.	3. Recipient's Catalog No.	
4. Title and Subtitle AIRBORNE INFRARED POLARIMETER		5. Report Date October 1972	
		6. Performing Organization Code	
7. Author(s) D.L. Coffeen, J. Hämeen-Anttila, R.H. Toubhans		8. Performing Organization Report No.	
9. Performing Organization Name and Address Lunar and Planetary Laboratory University of Arizona Tucson, Arizona 85721		10. Work Unit No.	
		11. Contract or Grant No. NAS5-21661	
12. Sponsoring Agency Name and Address Goddard Space Flight Center Greenbelt, Maryland 20771 Dr. W. Hovis, Code 652		13. Type of Report and Period Covered Final Project Report for period Sept 1971 thru September 1972	
		14. Sponsoring Agency Code	
15. Supplementary Notes			
16. Abstract <p>The AEROPOL infrared polarimeter was built for measurements between 1.1 and 3.5μ, with a 1°5 field of view, using a wire-grid polarization analyzer. A PbS detector is cooled by condensed Freon-13. The instrument operates under minicomputer control, giving a polarization least-squares solution each 2.5 seconds. AEROPOL was flown on the NASA CV-990 aircraft, in a remote-sensing study of terrestrial cloud particle sizes and shapes. (Submitted for publication in <u>Space Science Instrumentation</u>)</p>			
17. Key Words (Selected by Author(s)) polarization infrared instrumentation light scattering clouds		18. Distribution Statement	
19. Security Classif. (of this report) unclassified	20. Security Classif. (of this page) unclassified	21. No. of Pages 27	22. Price* \$ 350

*For sale by the Clearinghouse for Federal Scientific and Technical Information, Springfield, Virginia 22151.

**Details of illustrations in
this document may be better
studied on microfiche**

Airborne Infrared Polarimeter

D. L. Coffeen, J. Hämeen-Anttila, R. H. Toubhans*

(submitted 11 September 1972)

ABSTRACT

The AEROPOL infrared polarimeter was built for measurements between 1.1 and 3.5 μ , with a 1°5 field of view, using a wire-grid polarization analyzer. A PbS detector is cooled by condensed Freon-13. The instrument operates under minicomputer control, giving a polarization least-squares solution each 2.5 seconds. AEROPOL was flown on the NASA CV-990 aircraft, in a remote-sensing study of terrestrial cloud particle sizes and shapes.

INTRODUCTION

Passive remote sensing of incoherent electromagnetic radiation can at the very best monitor four different parameters as a function of wavelength, time, and scattering geometry and location. The four parameters can be expressed as (1) absolute intensity, (2) percentage linear polarization, (3) position angle of polarization and (4) percentage circular polarization. Most remote sensing of the earth has dealt with intensity alone. But all four parameters have potential significance. The percentage linear polarization can be particularly helpful in deducing the size, shape, and refractive index of suspended particles, especially when measured as a function of wavelength and phase angle (sun-particle-observer angle)^{1,2}.

Our scientific goal is the determination of particle phase and particle size in terrestrial cloud tops as viewed from above (from a satellite or

* The authors are with the Lunar and Planetary Laboratory of the University of Arizona, Tucson, 85721.

aircraft), of meteorological interest as well as for a test of polarization inversion techniques. The initial concept arose with Drs. Rasool and Hansen of the Goddard Institute for Space Studies. A prototype polarimeter (measuring percentage linear polarization and position angle of polarization) was designed and built at the Lunar and Planetary Laboratory, and flown on a series of flights of the NASA Convair 990 in January 1972. The data analysis and interpretation will be reported elsewhere³. This paper describes the instrument design, on-line processing techniques, calibrations, and general flight performance.

INSTRUMENT DESIGN

The following design goals were set for the AEROPOL instrument (a polarimeter measuring aerosols from an aeroplane):

- operation in the infrared between 1 and 4 μ (necessitated by contamination from molecular scattering at short wavelengths and thermal emission at long wavelengths, and by desire that wavelength be comparable to cloud particle sizes, and that measurements be made in wavelength regions of differing amounts of particle absorption).
- pointable (in order to vary the scattering geometry, to generate a curve of polarization versus phase angle while tracking a given region).
- field-of-view less than 2° (to avoid excessive angular smoothing of rainbow peaks, glories, etc.)
- polarization accuracy $\pm \frac{1}{4}$ % for clouds of intermediate albedo.

- on-line polarization analysis and operational control.
- photographic record of target.

Figure 1 shows the completed system.

OPTICAL

Figure 2 is an assembly drawing of the polarimeter, including the optical elements. Light from below passes through a 3 mm thick protective window of GE125 fused silica and then through a rotating Perkin-Elmer wire grid polarizer⁴ (2880 gold wires/mm deposited on AgBr) forming the entrance pupil of 21.5 mm. The wire grid substrate is significantly wedge-shaped as supplied by the factory (~16 arcminutes in this case); a compensating wedge of 1.0 mm thick Schott IRG9 glass was mounted with this analyzer to minimize displacement of the field-of-view. Maximum image displacement in the focal plane is 0.13 mm.

The objective lens rotates with the wire-grid analyzer; it was cut from crystalline MgF_2 by Continental Optical Co., with the fast axis perpendicular to the optic axis and mounted at 45° to the analyzer principal axis. Thus it serves as a "pseudo-depolarizer"⁵ for the highly-polarized light incident from the analyzer, with a retardation which varies with wavelength and with path length through the lens. The central lens thickness (25.4 mm) is near the minimum value to give sufficient depolarization for the several filter passbands. The success is shown by the low values ($\leq 1\%$) of instrumental polarization found for incident unpolarized radiation. A disadvantage of this analyzer/depolarizing objective lens combination is that the lens has different back focal distances for the ordinary and extraordinary rays. This difference

(4.9 mm in the present case) was acceptable here because of the relatively large and uniformly illuminated field of view. The objective lens is biconvex, $\sim f/6.8$, shaped for minimum spherical aberration.

The converging beam then falls on a two-bladed reflective chopper (a single piece of gold-coated plate glass). During the dark phase the light beam falls on a 3M 101-C10 Black Velvet paint surface, while the detector sees itself (the coldest point in the instrument) in a concave spherical gold-coated mirror.

The reflected beam passes through one of five different interference filters, described in Table I. Figure 3 shows the normalized passbands as weighted by the incident spectrum, the instrument transmittance, and the detector response. The corresponding effective wavelengths (in this case the "isopolaral" wavelengths λ_{ip}) are given in Table I. The physical thicknesses of the several filters are tailored to approximately achromatize the focal distance.

Table I. Filter Characteristics

λ_{peak}	T_{peak}	λ_{ip}	Amplifier Gain
1.27 μ	0.77	1.236 μ^*	1
1.64	0.71	1.595	1
2.28	0.72	2.222	1.7
3.18	0.67	3.084	14
3.43	0.75	3.379	21

* Short-pass filter; the silicon Fabry lens forms the short-wavelength side of the passband.

Next in sequence is the 4.0 mm focal-plane aperture, restricting the field-of-view to 1.5° , followed by the evacuated dewar, incorporating a sapphire window, a plano-convex silicon Fabry lens, and the PbS detector. The lens images the entrance pupil onto the 0.5 mm x 0.5 mm detector surface; the lens is antireflection coated both sides, and is separated from the detector by 1.85 mm. The Fabry image quality and the instrumental polarization effects are discussed in the Calibration Section. Santa Barbara Research Center supplied the detector-dewar combination, and mounted the lens to specification. The detector alone has a peak D-star at 2.8μ of $4.2 \times 10^{11} \text{ cm Hz}^{\frac{1}{2}} \text{ watt}^{-1}$, when operated at 193°K with a 90 Hz chopping frequency, viewing a 295°K background over 2π steradians.

For visual tracking a second port is located adjacent to the infrared window. Light passes through a pressure window; then a 90° reflection, through a 1:1 riflescope with reticle, and to a Nizo S-56 super-8 mm single lens reflex movie camera. The resultant field-of-view is 10° . One Kodachrome II film frame is recorded at each rotation of the analyzer for which polarization data is taken.

MECHANICAL

Figure 4 is a view of the AEROPOL instrument interior. The basic instrument is a circular cylinder mounted in a 14° "side-looking" window of the NASA CV-990, with an IR window pointing downwards. The entire cylinder can be manually rotated about its axis of symmetry, which is horizontal, to provide views forward and aft over the range $\pm 70^\circ$ from the nadir. This rotation permits selection of the scattering angle, for a given flight path; alternatively it permits a limited tracking ability for isolated clouds on the flight path.

The rotation employs an outer ball bearing, and uses a double O-ring seal of silicone rubber. The pressure differential between interior and exterior is typically 500 mb, the air temperature differential 75°C.

Two motors are employed. A hysteresis-synchronous motor drives the chopper blade at 83 chops per second, and, through a linkage of gears, the analyzer/depolarizer/lens unit at 0.48 seconds per revolution. Stainless steel gears are lubricated with a mixture of machine oil and low temperature grease. A stepper motor drives the filter wheel rotation at 9 ms per step until the desired filter position is achieved (16 steps between filters). The chopper mirror was readily positioned and checked dynamically by using a stroboscope triggering on the computer sample pulses.

The detector with cold shield and Fabry lens is mounted in a small glass dewar which is potted in a metal can with RTV compounds. A miniature cylindrical Joule-Thompson open-loop cryostat is press fitted into the dewar inner finger, with its outlet tube immediately behind the detector platform. A conductive coating on this inner finger serves to electrically ground the liquid coolant spray to the metal cryostat tubing. Freon-13 gas at 225 psi is supplied to the cryostat, with a consequent flow rate of approximately 1 liter per minute. A 25-minute initial cool-down is done at 250 psi. The Freon-13 is dried by filtering through a 4.4" length of granular molecular sieve. An in-line flowmeter is especially useful as an indicator of leaks in the system.

ELECTRONIC

The electronic system is relatively complicated by the need for on-line reductions. These were necessitated by the exploratory nature of the experiment combined with a flight program limited in duration and the goal of getting the most knowledge from the initial flights. In addition, the instrument had to be made to a great extent automatic to free the observer for manual tracking of the cloud targets. To achieve these goals, and to allow for fast changes if needed during the flights, the system was built around a Data General Corporation Nova 1200 minicomputer as instrument controller and data processor.

Figure 5 shows a block diagram of the electronics system. The detector bias is adjustable between 0 and 50 V to set the sensitivity of the detector. This voltage is applied across the PbS photoconductive detector wired in series with a 0.6 Megohm load resistor, through an RC-network to protect detector from voltage transients. The AC signal from the detector, which is proportional to the incident intensity, is preamplified by an Infrared Industries Model 650A low noise amplifier and then amplified by a programmable gain amplifier, the gains of which are set to give approximately equal signals with each of the optical filters, for a typical cloud. These gains, which are selected by reed switches at the filter wheel, are shown in Table I.

The 12-bit analog to digital converter has four program selectable inputs. One is used to sample the detector signal synchronously with the light chopper rotation, to get a reading during each light and dark position (i.e., one reading each 6 msec.). The other three inputs are used to read the filter wheel position and the instrument pointing angle from the outputs of two precision potentiometers, and the temperature inside the instrument from a resistor-thermistor voltage divider.

The position of the rotating polarization analyzer is sensed by a magnetic

pick-up, which gives a synchronization pulse once every revolution of the analyzer.

All timing is derived from the computer's 1kHz crystal controlled oscillator. From this, and the synchronization pulses, the program creates a 55.56 Hz signal to drive the synchronous chopper/analyzer motor, the filter wheel stepper motor pulses, the camera triggering pulses, and the 1 second pulses to update a 24 hour software clock.

The peripherals include a long persistence oscilloscope used as an X-Y CRT display, and^a teletypewriter. The CRT can be switch selected to show the analog detector output, the digitized detector signal fed back from the computer, or the analyzer synchronization signal. Measurement results are punched on paper tape and printed by the teletypewriter, and also recorded on magnetic tape through the NASA CV-990 data acquisition system as a back-up.

Operator input to the system is through the teletypewriter keyboard to set initial clock time and parameters for the automatic measuring sequence, and through the computer sense switches for control of the motors and for start of measurement.

ON-LINE PROCESSING

The assembly language program for the NOVA computer was created using a cross-assembler running on a large scale CDC 6400 computer. This allowed us to use cards rather than paper tape for the source program, which simplified editing and gave the power of a higher level assembler than is available for the NOVA with its 4096-word memory.

The program is approximately 950 statements long. It is loaded in the core twice, together with simple operator controlled routines to reload the program from the copy in case of program trouble, and to print out the

differences between the two copies for debugging purposes.

A simplified flow chart of the program is in Figure 6. All timing, input-output and control functions, and the cumulation of measured data, are handled by interrupt routines. The background program consists of the updating of the output files.

During a measurement sequence, the filter is automatically changed after a predetermined time of data cumulation. After a sequence of six filters, the results are printed and punched, time-shared with the next measurement sequence.

All calculations are done using integer arithmetic, and tables for trigonometric functions. This was possible as the range of the input data was predictable because of the limits of the analog-to-digital converter, and allowed us to use appreciably less core memory and to make the measurements faster than with floating point arithmetic.

Each "dark" reading is stored to be subtracted from the following "light" reading, resulting in 40 difference readings corresponding to the 80 samples each revolution of the analyzer. The signal corresponding to a partially linearly polarized input is an offset double sine-curve, which can be represented by:

$$S(\theta) = A_0 + A_2 \cos 2\theta + B_2 \sin 2\theta$$

where θ is the angle of rotation of the analyzer, and A_0 , A_2 , B_2 are constants dependent on the intensity and polarization of the incoming radiation. The on-line program solves for A_0 , A_2 , and B_2 by cumulating the difference readings into three storage locations, one representing the cumulative sum of all the differences, and the other two the sum of the differences multiplied by the cosines or sines, respectively, of two times the angular position of the analyzer. After a complete measurement at one filter, these sums are divided

by the total number of samples, and the last two sums additionally by 2, i.e. A_0 , A_2 , and B_2 are solved from:

$$A_0 = \frac{1}{n} \sum_{i=1}^n D_i$$

$$A_2 = \frac{1}{2n} \sum_{i=1}^n D_i \cos 2\theta_i$$

$$B_2 = \frac{1}{2n} \sum_{i=1}^n D_i \sin 2\theta_i$$

A_0 is proportional to the intensity, and A_2/A_0 and B_2/A_0 represent the fractional polarization in component form. These are printed out, multiplied by suitable constants to avoid decimal numbers (A_0 by 2 to keep full scale intensity readings somewhat below 10000 to always limit the output to four digits, each fraction by 1000 which then represents 100% polarization along one component axis). In addition to these three numbers for each of the six filters, the print-out contains local time and a record of operator-selectable parameters. A seventy-two second sample of on-line output is shown in Figure 7.

During off-line processing, data are punched on cards from the paper tape to allow easy editing. Further processing converts all housekeeping data to proper physical units, and includes calibration corrections.

CALIBRATIONS

Figure 8 shows the angular response pattern of the completed instrument to unpolarized light at 2.22 μ ; the pattern is similar at other wavelengths. It was measured by observing a quartz-halogen lamp point source at 0.2 spacing in the far field.

The polarization introduced by the instrument was measured as above; the lamp polarization was removed by observing the lamp in two positions 90° apart. Figure 9 shows the angular pattern of instrumental polarization at 2.22 μ .

Integrated over the field of view the instrumental polarization is rather small, and can be well calibrated. The integrated values were measured by observing a ground silica plate illuminated from behind by the lamp, and rotating the lamp through 90°. The integrated polarizations are given in Table II.

Table II. Instrumental Polarization.

<u>$\lambda(\mu)$</u>	<u>P(%)</u>	<u>$\theta(\text{deg.})$</u>
1.24	0.60	73
1.60	0.78	64
2.22	0.97	82
3.08	0.81	79
3.38	--	--

For a perfect instrument the angular response pattern would be exactly uniform over a circular region, corresponding to the circular focal plane aperture, and zero outside this. The instrumental polarization would be identically zero everywhere. The measured imperfections may be traceable to aberrations in the Fabry lens and nonuniform detector sensitivity. The Fabry lens is designed to image the entrance pupil onto the detector. As the objective lens assembly rotates, the entrance pupil has negligible runout, but there is a small angular wobble of the field of view (0.13 mm in the focal plane).

This can create an intensity modulation of the signal, although it tends to disappear in the polarization solution, since the angular wobble has twice the period of the polarization modulation. The single Fabry lens element will show spherical and chromatic aberration; the entrance pupil will not be well-

focussed on the detector. Therefore the distribution of light on the detector will depend somewhat on the target and on the illumination geometry of the Fabry lens. Also the polarization aberration of the objective lens gives imperfect focal-plane images. Finally, a significant source of instrument polarization may simply be incomplete depolarization of the high polarization introduced by the analyzer, and consequent interaction with the polarization-sensitive components (chopper mirror, Fabry lens, detector).

Some real-time calibrations are possible as part of the observing sequences, by using three insertable slides located in front of the analyzer/objective lens. The outermost slide is a dark shutter; this permits measurement of any background intensity levels appearing as a difference between "dark" and "light", particularly thermal emission within the instrument. The next slide contains an array of 21 microminiature incandescent lamps, which gives an intensity reference and a check on instrumental polarization. The inner slide is an infrared polarizer, identical to the analyzer, used for checking the instrument response to large polarizations.

FLIGHT PERFORMANCE

Successful observing runs were made over a wide variety of cloud types during a series of ten airplane flights over the northwest U. S. coast, the central U. S., the Caribbean, and the equatorial western Atlantic.

Some instrument problems were experienced during the initial flights due to unexpectedly high cooling of the instrument by the air flow. The chopper motor was being overloaded and running asynchronously, caused by thickening of the lubricant on a set of helical gears in the drive train. Also an operational amplifier went into oscillation below 0°C. The addition of localized resistive heaters solved both problems.

Other system components worked very well; we were particularly pleased with the simple and faultless operation of the open-loop Freon-13 cryostat, and with the real time feedback made possible with the on-line processor.

ACKNOWLEDGMENTS

This instrument was funded by NASA Goddard Space Flight Center, through Dr. Hovis, under NAS5-21661. At the University of Arizona, E. Roland assisted in the optical design and M. Arthur fabricated the electronics and participated in the data flights; Baker and Castillo helped with instrument calibrations. Santa Barbara Research Center was very helpful with the technology of the detecting and cooling systems. We particularly appreciate the cooperation of Earl Petersen and the flight crew and staff of the NASA/Ames Research Center Convair 990 program.

REFERENCES

- ¹ D. L. Coffeen, Astron. J. 74, 446 (1969).
- ² J. Hansen and A. Arking, Science 171, 669 (1971).
- ³ D. L. Coffeen and J. Hansen, J. Atmos. Sci. (in preparation).
- ⁴ "Wire Grid Polarizers and Mounting Kits", Perkin-Elmer Spectroscopy Data Sheet D-459.
- ⁵ Shurcliff, W. A., 1962, Polarized Light, Harvard Univ. Press, p. 107.

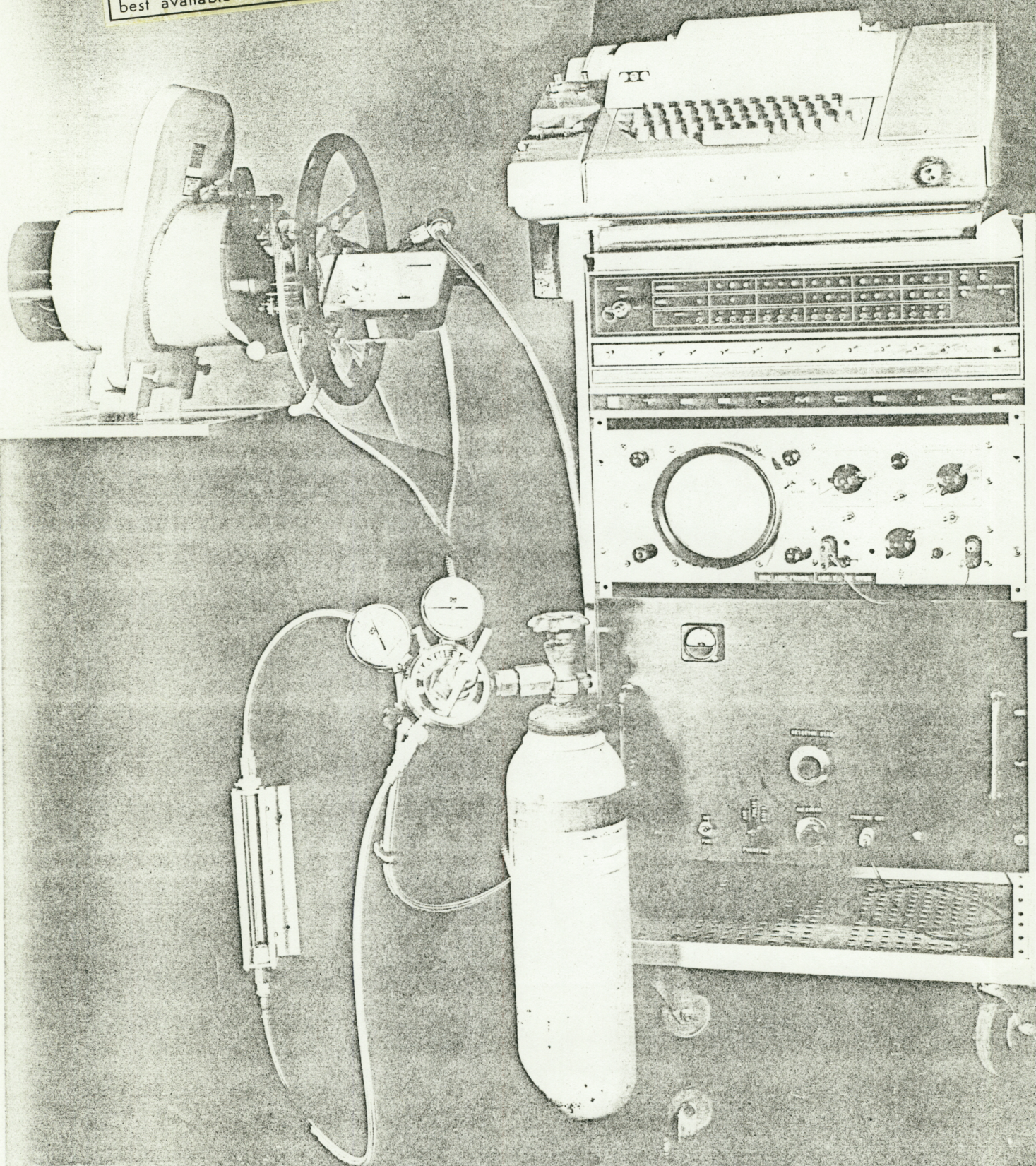
CAPTIONS

- Figure 1. AEROPOL system, including infrared polarimeter, power supplies, NOVA minicomputer controller/processor, teletype input/output, oscilloscope displaying chopped waveform, and Freon-13 coolant.
- Figure 2. Assembly drawing of polarimeter, including calibration slides, rotating analyzer/depolarizer/objective lens assembly, chopper mirror, filter wheel, dewar, Freon-13 cryostat, and motors.
- Figure 3. Effective passbands. Relative instrument response to a typical cloud spectrum is plotted vs. wavelength. The five bandpasses are normalized at peak response.
- Figure 4. Instrument detail. The basic structure consists of four mounting plates hung on Invar rods, giving ready access to all components. This entire assembly is isolated from the outer container by O-ring mounts, with rubber bushings on the motor shafts.
- Figure 5. Electronics block diagram.
- Figure 6. On-line program flow chart.
- Figure 7. 72-second sample of on-line output, observing cloudbow region on thick cumulus layer, 29 January 1972, Carribean. Numbers on the left give intensity and two polarization components $1000 p \cos 2\theta$, $1000 p \sin 2\theta$, every 2.5 seconds. Numbers on the right give instrument temperature, filter code, number of analyzer revolutions, instrument look angle, and time. Each measure of polarization is the least-squares sinusoidal fit for 200 data points.

Figure 8. Angular response pattern at 2.22μ . Instrument response to a point source is plotted as a function of source azimuth and elevation in degrees.

Figure 9. Instrumental polarization pattern at 2.22μ . Percentage polarization P and position angle θ are plotted for the angular region of high sensitivity shown in Fig. 8. Azimuth and Elevation are marked in 0.2 steps.

Reproduced from
best available copy.



Reproduced from
best available copy.

FIG. 10-12-13A

FIG. 10-12-13B

FIG. 10-12-13C

FIG. 10-12-13D

FIG. 10-12-13E

FIG. 10-12-13F

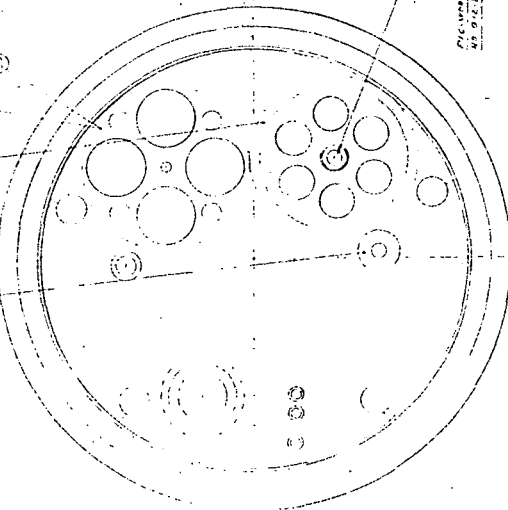
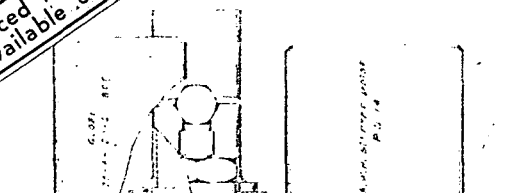
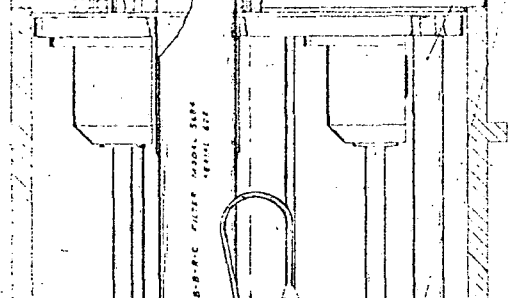
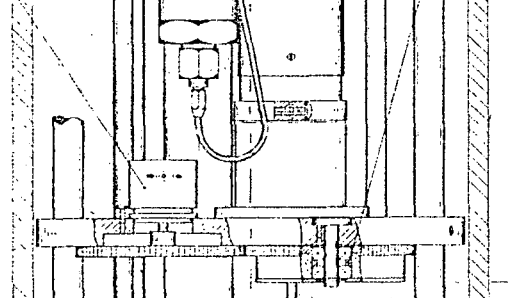
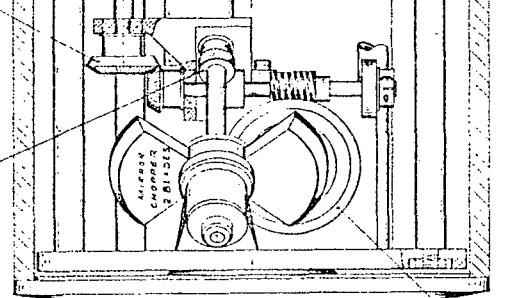


FIG. 10-12-13A



SECTION A-A

SECTION B-B

SECTION C-C

SECTION D-D

SECTION E-E

SECTION F-F

SECTION G-G

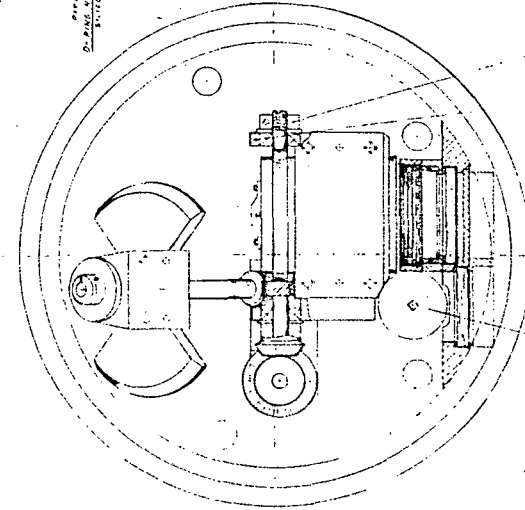
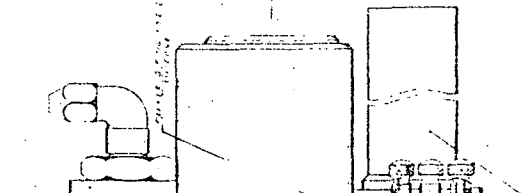
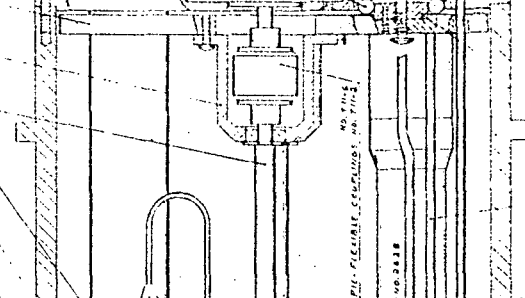
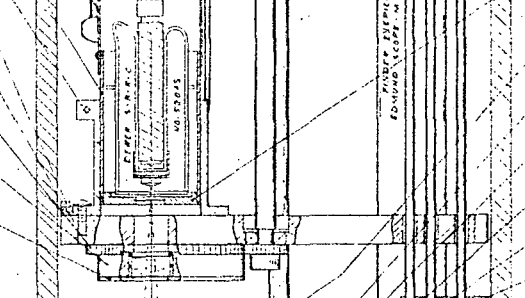
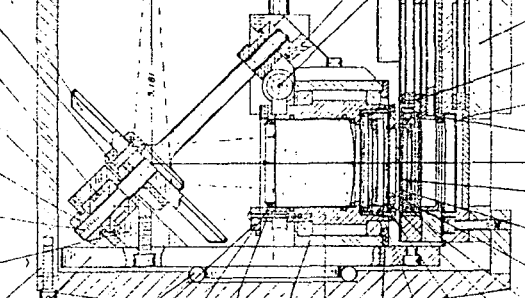


FIG. 10-12-13A



SECTION A-A

SECTION B-B

SECTION C-C

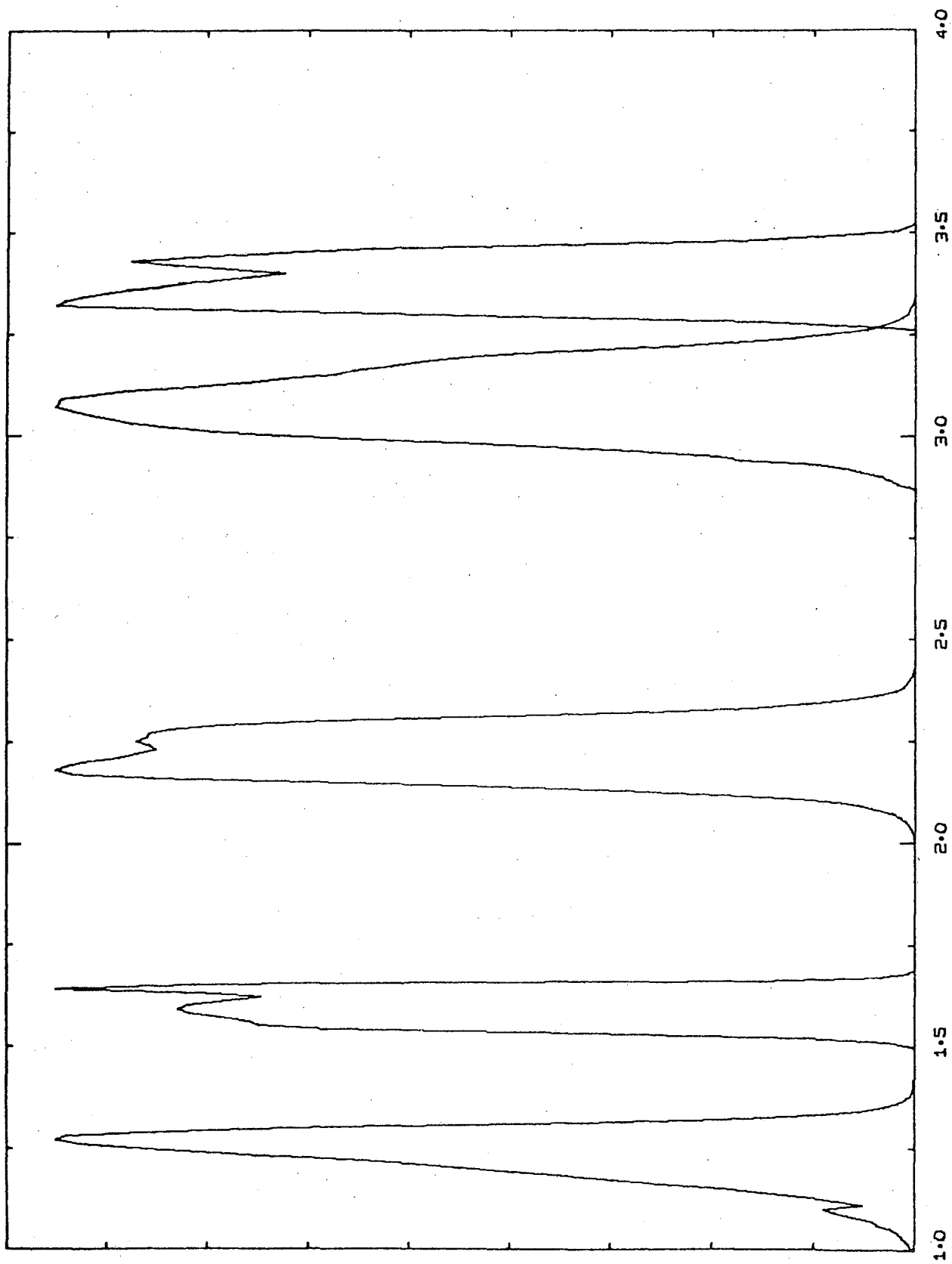
SECTION D-D

SECTION E-E

SECTION F-F

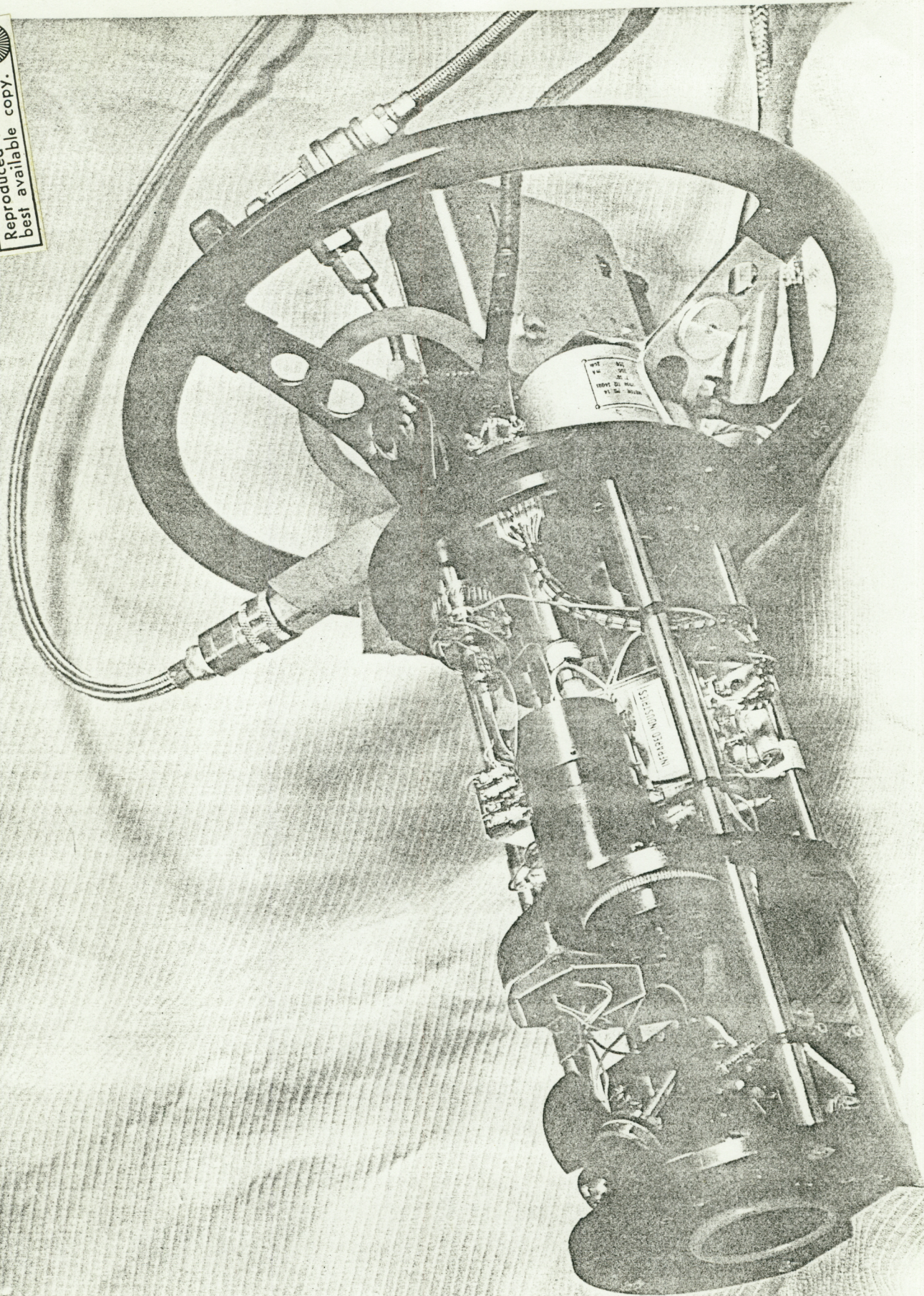
SECTION G-G

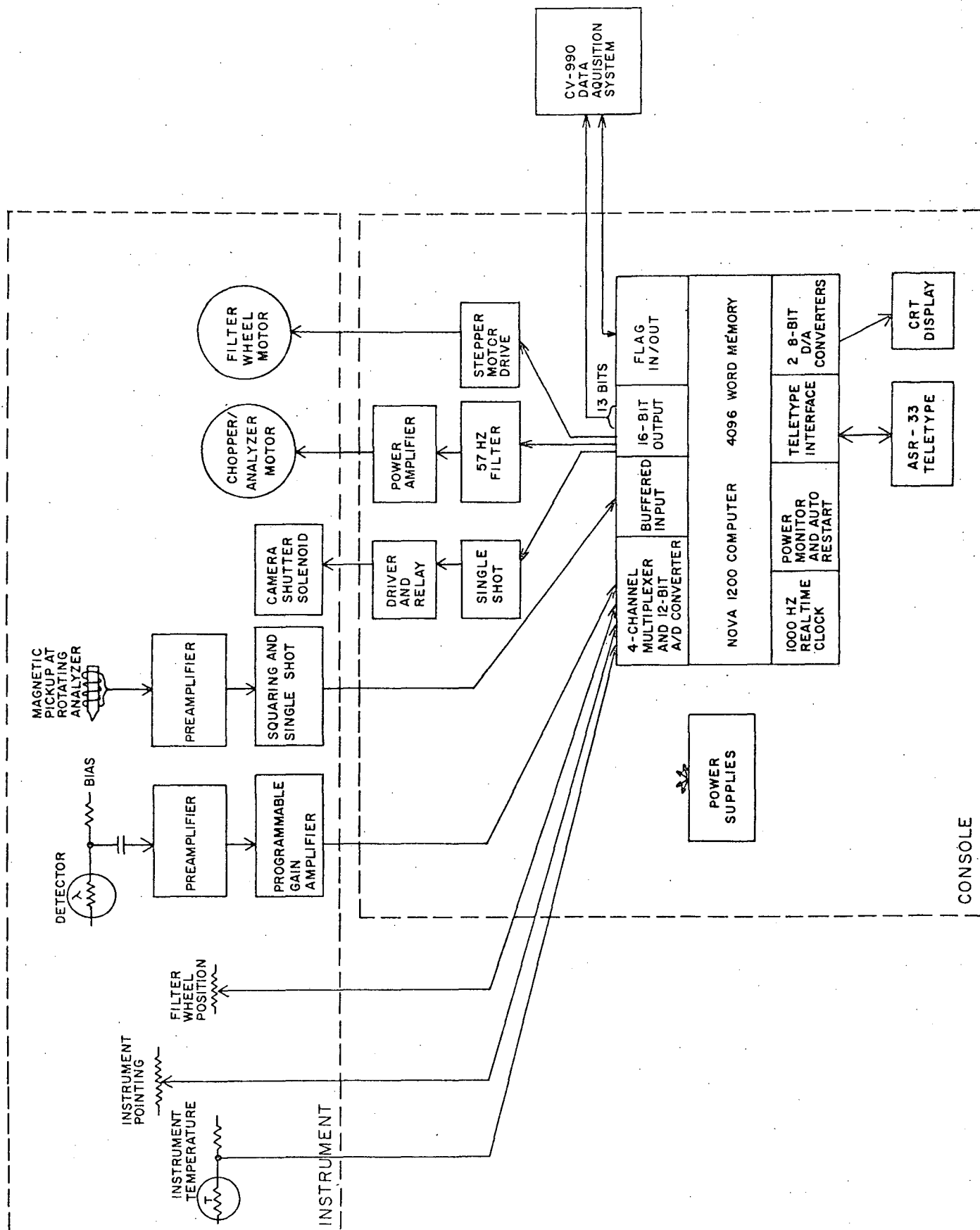
LUNAR & PLANETARY LAB.	
UNIVERSITY OF TORONTO	
PROJECT NO.	10-12-13
DATE	1964
BY	W. J. G. & J. G.
CHECKED BY	W. J. G. & J. G.
APPROVED BY	W. J. G. & J. G.



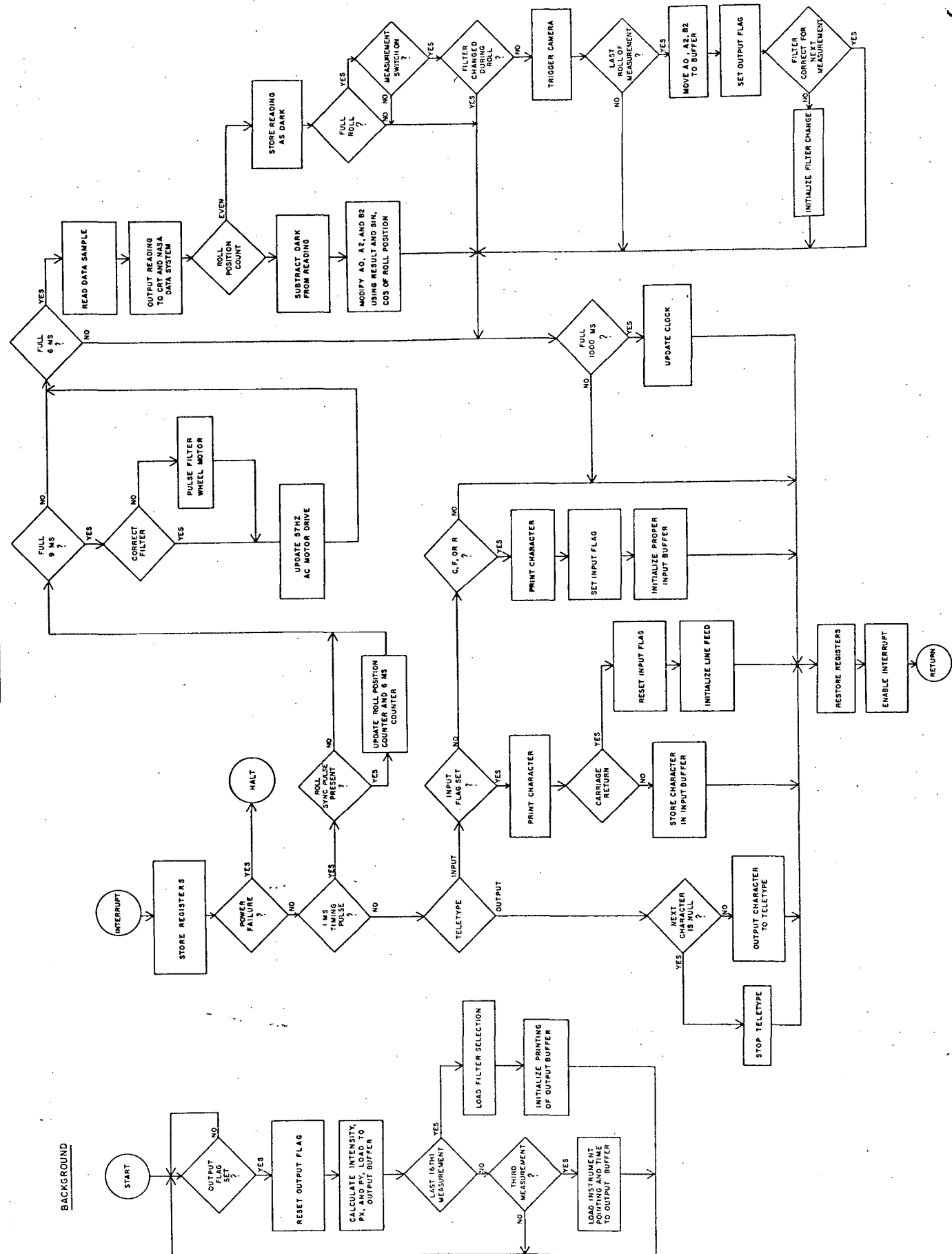
WAVELENGTH (MICRONS)

Reproduced from
best available copy.





INTERRUPT PROCESSING



2390-001 001 2338-002 000 2293-002 001	T1249 F3 R05 P1688 16:23:47
2259-000 000 2213 000 000 2185 000-000	
2215-000-000 2177-012-008 2132-032-030	T1247 F3 R05 P1870 16:24:00
2195-045-049 2120-050-048 2149-052-057	
2056-051-060 2094-050-061 2220-041-053	T1244 F3 R05 P2006 16:24:13
2177-030-041 2072-024-032 2086-018-028	
1996-014-021 1760-012-018 1691-009-017	T1244 F3 R05 P2183 16:24:26
1784-007-016 1819-004-005 1889-005-004	
1989-001-000 1936-002 003 1795-000-000	T1239 F3 R05 P2375 16:24:39
1969 001-001 1892 002 001 1827 004 005	

